



LETTER

# $\pi$ -kink propagation in the damped Frenkel-Kontorova model

To cite this article: K. Alfaro-Bittner *et al* 2017 *EPL* **119** 40003

View the [article online](#) for updates and enhancements.

## Related content

- [The mathematics behind chimera states](#)  
O E Omel'chenko
- [Coexisting coherent and incoherent domains near saddle-node bifurcation](#)  
V. K. Chandrasekar, R. Suresh, D. V. Senthilkumar et al.
- [On the bifurcation to moving fronts in discrete systems](#)  
N J Balmforth, T M Janaki and A Kettapun

# $\pi$ -kink propagation in the damped Frenkel-Kontorova model

K. ALFARO-BITTNER<sup>1</sup>, M. G. CLERC<sup>2</sup>, M. A. GARCÍA-ÑUSTES<sup>1</sup> and R. G. ROJAS<sup>1</sup>

<sup>1</sup>*Instituto de Física, Pontificia Universidad Católica de Valparaíso - Casilla 4059, Valparaíso, Chile*

<sup>2</sup>*Departamento de Física, Facultad de Ciencias Físicas y Matemáticas, Universidad de Chile  
Casilla 487-3, Santiago, Chile*

received 2 June 2017; accepted in final form 3 October 2017

published online 6 November 2017

PACS 05.45.-a – Nonlinear dynamics and chaos

PACS 05.45.Xt – Synchronization; coupled oscillators

**Abstract** – Coupled dissipative nonlinear oscillators exhibit complex spatiotemporal dynamics. Frenkel-Kontorova is a prototype model of coupled nonlinear oscillators, which exhibits coexistence between stable and unstable state. This model accounts for several physical systems such as the movement of atoms in condensed matter and magnetic chains, dynamics of coupled pendulums, and phase dynamics between superconductors. Here, we investigate kinks propagation into an unstable state in the Frenkel-Kontorova model with dissipation. We show that unlike point-like particles  $\pi$ -kinks spread in a pulsating manner. Using numerical simulations, we have characterized the shape of the  $\pi$ -kink oscillation. Different parts of the front propagate with the same mean speed, oscillating with the same frequency but different amplitude. The asymptotic behavior of this propagation allows us to determine the minimum mean speed of fronts analytically as a function of the coupling constant. A generalization of the Peierls-Nabarro potential is introduced to obtain an effective continuous description of the system. Numerical simulations show quite fair agreement between the Frenkel-Kontorova model and the proposed continuous description.

Copyright © EPLA, 2017

**Introduction.** – Nonlinear oscillators such as the pendulum have played a primary role in the understanding of complex dynamics since the dawn of modern science [1,2]. Even a simple two-oscillators coupled system shows interesting behavior such as synchronization [3]. A chain of coupled oscillators to nearest neighbors also can present a rich spatiotemporal dynamics [3–5], such as phase turbulence [4], synchronization [3], defects turbulence [6], random occurrence of coherence events [7], defect-mediated turbulence [8], spatiotemporal intermittency [9], quasiperiodicity in extended system [10] and coexisting of coherent and incoherent behavior, known as chimera states [11]. A prototype model of coupled nonlinear oscillators to nearest neighbors is the Frenkel-Kontorova model [12]. Figure 1 illustrates a chain of coupled pendulums. In the context of condensed matter, it is the simplest model that describes the dynamics of a chain of particles interacting with the nearest neighbors under the influence of an external periodic potential [12,13]. It has been used to describe several nonlinear phenomena such as solitons, kinks, breathers, and glass-like behavior. Likewise, this model has been used to describe cluster of atoms in DNA-like chain, spin in magnetic chain, fluxon

in coupled Josephson junctions and plastic deformations in metals (see textbook [12] and references therein). The Frenkel-Kontorova model exhibits coexistence between a stable extended state and an unstable one. The solution that connects both is called the  $\pi$ -kink [14], which corresponds to a topological particle-type solution. As a matter of fact, a rich domain dynamics can emerge between  $\pi$ -kink solutions. In dissipative systems,  $\pi$ -kinks are also known as front solutions, or wavefronts [15–17], depending on the physical context where they are considered. Front dynamics occurs in a variety of systems ranging from biology to physics [18,19]. Interfaces between metastable states can also appear in the form of propagating fronts, leading to a rich spatiotemporal dynamics [20,21]. Most of the theoretical studies of fronts propagation have been achieved considering the continuous limit [15,18,21]. At this limit, the fronts propagate as a rigid solid with a speed determined by the initial conditions. However, recently, in coupled micropillar laser with saturable absorber has been observed the propagation of self-pulsating states [22,23]. Hence, the nonlinear waves propagation in these optical oscillators is not correctly well contained in the continuous description.

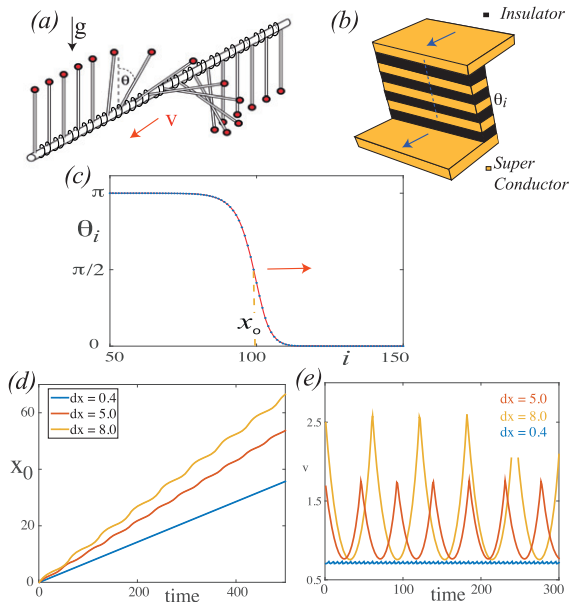


Fig. 1: (Color online) Frenkel-Kontorova model. (a) Schematic representation of a chain of dissipative coupled pendulums, a  $\pi$ -kink solution. (b) Representation of a coupled Josephson junctions. (c) Instantaneous profile of a  $\pi$ -kink of eq. (1), dots and solid line represent numerical simulation values of  $\theta_i$  and their interpolated curve, respectively;  $x_0$  accounts for the front position. (d) Temporal evolution of the front position  $x_0(t)$  with  $\omega = 1$  and  $\mu = 20$ . The upper (yellow), middle (orange) and lower (blue) lines correspond to different discreteness  $dx = 1\sqrt{\kappa}$ ,  $dx = 10$ ,  $dx = 7$ , and  $dx = 3$ , respectively. (e) Temporal evolution of the front speed  $\dot{x}_0(t)$  with  $\omega = 1$  and  $\mu = 6$ . The upper (yellow), middle (orange) and lower (blue) lines correspond to  $dx = 5$ ,  $dx = 2$ , and  $dx = 0.1$ .

The aim of this letter is to investigate the  $\pi$ -kinks propagation into an unstable state in the Frenkel-Kontorova model with dissipation as a prototype model of nonlinear waves propagation in discrete media. We show that unlike point-like particles  $\pi$ -kinks spread in a pulsating manner. Using numerical simulations, we have characterized the shape of the  $\pi$ -kink oscillation. Different parts of the front propagate with the same mean speed, oscillating with the same frequency but different amplitude. The asymptotic behavior of this propagation allows us to determine the minimum mean speed of  $\pi$ -kinks analytically. To figure out this propagation phenomenon, we generalize the notion of the Peierls-Nabarro potential to obtain an effective continuous description of the system. Numerical simulations show quite fair agreement between the Frenkel-Kontorova model and the proposed continuous description.

**Model.** – Let us consider a chain of dissipative coupled pendulums, which is described by the damped Frenkel-Kontorova equation,

$$\ddot{\theta}_i = \omega^2 \sin \theta_i - \mu \dot{\theta}_i + \kappa (\theta_{i+1} - 2\theta_i + \theta_{i-1}), \quad (1)$$

where  $\theta_i(t)$  is the angle formed by the pendulum and the vertical axis in the  $i$ -position at time  $t$ ,  $\theta_i = 0$  ( $\theta_i = \pi$ ) corresponds to the upside-down (upright) position of the pendulum. We have considered this choice of the origin of the angle to facilitate the numerical study of  $\pi$ -kinks.  $i$  is the index label the  $i$ -th pendulum,  $\omega$  is the pendulum natural frequency,  $\mu$  accounts for the damping coefficient, and  $\kappa$  stands for the coupled interaction between adjacent pendulums. Figure 1(a) shows the chain of dissipative coupled pendulums schematically. Notice each pendulum is coupled to the nearest neighbors. The model eq. (1) can be also applied to coupled identical Josephson junctions [24,25]. A scheme of this system is depicted in fig. 1(b), where  $\theta_i(t)$  accounts for the phase difference between the wave function of each superconductors in the  $i$ -th junction. The parameter  $\omega^2$  stands for the superconductor current in the junctions, and its value is determined by the particular characteristics of the junction. The parameter  $\mu$  accounts for the normal current and the parameter  $k$  accounts for the coupling between nearest junctions. In the continuous limit, considering  $\theta(x, t) = \lim_{dx \rightarrow 0} \theta_i(t)$ ,  $x = \lim_{dx \rightarrow 0} idx$ ,  $\kappa \rightarrow \infty$ , and  $\kappa dx^{-2} \rightarrow D$  ( $D$  is a finite constant that accounts for the diffusion coefficient), eq. (1) becomes in the damped sine-Gordon equation.

The dissipative model, eq. (1), can be rewritten in the following manner:

$$\mu \dot{\theta}_i = -\frac{\delta F}{\delta \theta_i}, \quad (2)$$

where the Lyapunov function  $F$  has the form

$$F[\theta_i, \dot{\theta}_i] \equiv \sum_{i=0}^N \left[ \frac{\dot{\theta}_i^2}{2} + \omega^2 \cos \theta_i + \kappa \frac{(\theta_{i+1} - \theta_i)^2}{2} \right]. \quad (3)$$

Hence, the dynamics of eq. (1) is characterized by the minimization of function  $F$  when  $\mu \neq 0$ .

**$\pi$ -kink solutions.** – Equation (1) has two extended equilibria, the upright and the upside-down position of pendulums. The upright (upside-down) position of pendulums is a stable (unstable) equilibrium. Hence, as a result of the initial conditions, the chain of dissipative coupled pendulums can show domains of upright or upside-down pendulums. A domain wall which connects upright and upside-down domains corresponds to a  $\pi$ -kink state [14]. Indeed, this front solution is characterized by a jump in  $\pi$  at the angle. Figure 1(a) illustrates a  $\pi$ -kink solution for this chain.

Because the upright pendulums are stable the  $\pi$ -kink solution propagates such that an upside-down pendulum can rotate to minimize the Lyapunov potential  $F$ . Front position is a fundamental concept in the characterization of domain walls as particle-type solutions and their respective dynamics. In the continuous limit, the front position,  $x_0$ , corresponds to the spatial location where the front exhibits its greater spatial variation. In the discrete case, the front position is defined using its spatial location in the

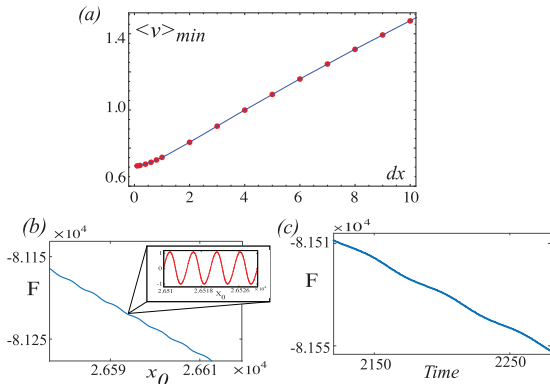


Fig. 2: (Color online)  $\pi$ -kink propagation in the Frenkel-Kontorova model with dissipation, eq. (1). (a) Front minimal mean speed  $\langle v \rangle_{min}$  as a function of the discreteness parameter  $dx = 1/\sqrt{\kappa}$ . Dots (red) are obtained by means of numerical simulations of eq. (1) with  $\omega = 1.0$  and  $\mu = 2.0$ . The solid line is obtained by using formulas (8) and (9). Lyapunov function, expression (3), vs. front position (b) and vs. time (c) obtained by numerical simulations of eq. (1) for the same parameters and  $dx = 5.0$ . Inset: Lyapunov function computed in a reference system moving with the mean speed of front, the co-mobile system.

corresponding continuous limit. In the continuous limit, the front position  $\theta(x, t)$ , corresponds to a horizontal position of the pendulum,  $\theta(x_0, t) \equiv \pi/2$ . More precise, the front position of the discrete chain of pendulums,  $x_0(t)$ , is defined by the spatial location of the intersection between the interpolated curve of  $\theta_i(t)$  and the horizontal pendulum (cf. fig. 1(c)). This position does not generally coincide with a precise point in the lattice. Figures 1(d) and (e) show, respectively, front position and speed ( $\dot{x}_0$ ) as a function of time for different values of coupling  $\kappa$  obtained from numerical simulations of eq. (1). Numerical simulations were conducted using finite differences method with a fourth-order Runge-Kutta algorithm and specular boundary conditions. As a matter of fact, the speed of propagation of the  $\pi$ -kink is oscillatory with a well defined average speed,  $\langle v \rangle$ . When decreasing the coupling  $\kappa$ ,  $\langle v \rangle$ , amplitude  $\eta$  and frequency  $\Omega$  of oscillation increases (cf. fig. 1). The oscillations exhibited by the speed are non-harmonic. Figure 2(a) shows  $\langle v \rangle$  as a function of the discreteness  $dx \equiv 1/\sqrt{\kappa}$ . For large discreteness, the speed increases linearly.

From a numerical  $\pi$ -kink solution of the Frenkel-Kontorova model with dissipation, eq. (1), we have computed the Lyapunov function  $F[\theta(x, x_0(t))]$  as a function of  $x_0$  or time. Figure 2(b) shows evolution of the Lyapunov function vs. the front position  $x_0$ . It is clear that the Lyapunov function decreases with time in an oscillatory manner (see fig. 2(c)).

Typically, the assumption that the front behaves as a point-like particle simplifies the analysis by reducing the whole front dynamics to a single point, the front position  $x_0(t)$ . That is, the point  $x_0(t)$  gives all the information

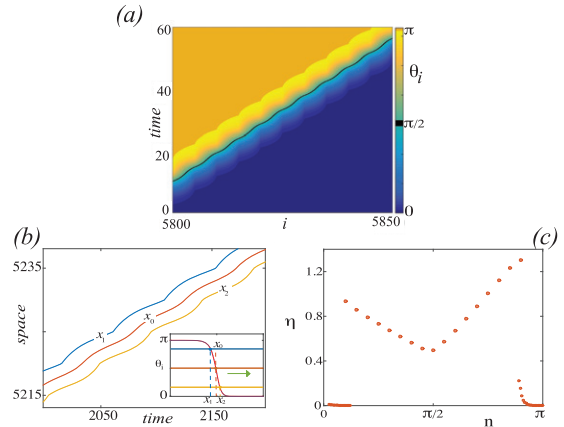


Fig. 3: (Color online) Front propagation into an unstable state in the Frenkel-Kontorova model with dissipation eq. (1). (a) Spatiotemporal diagram of  $\pi$ -kink solution of model (1) with  $\omega = 1.0$ ,  $\mu = 2.0$   $\kappa = 0.04$ . (b) Trajectories of three different points or cuts: above (upper yellow line), in (middle red line), and below (lower blue line) the front position. Inset: illustration of the different cuts under consideration. (c) Oscillation amplitude  $\eta$  of the front speed in different cuts.

about the dynamics of the whole structure. Surprisingly, the  $\pi$ -kink behaves as an extended object: each point of the solution shows an oscillatory dynamics with the same frequency but different amplitude. Figure 3(a) shows the spatiotemporal diagram of a  $\pi$ -kink solution. To understand the dynamical structure of the  $\pi$ -kink, we have monitored different cuts or values of the  $\pi$ -kink profile. To each cut, we can associate a  $x_n$  position, in analogy to the front position  $x_0$ , where  $n$  indexes the respective cut. Namely, the cuts  $x_n$  are defined by the spatial location of the intersection between the interpolated curve  $\theta_i(t)$  and an arbitrary value. This value ranges between the asymptotic values of the  $\pi$ -kink. Position  $x_n$  does not necessarily coincide with a precise point on the lattice. Note that the oscillation about the front position  $x_0$  is in anti-phase (see fig. 3). That is, the maximum oscillation of a point to the left of the front position coincides with the minimum oscillation of a point to the right. Figure 3(c) displays the amplitude of oscillation of the front speed,  $\eta$ , for different cuts. From this figure, we conclude that this amplitude is minimal at the front position, it increases as one moves away from the front position  $x_0$  and decays to zero abruptly at the kink tails. In the continuous limit, the  $\pi$ -kink propagates as a rigid solid with a well-defined speed. Hence, the observed dynamical behavior for the  $\pi$ -kink in the damped Frenkel-Kontorova model is a consequence of the discreteness of the system.

**$\pi$ -kink mean speed.** – Initial conditions determine the speed of propagation of a front into unstable states [18]. When initial conditions are bounded, after a transient period, two counterpropagative fronts emerge with a given speed, the minimum speed. When the so-called linear criterion determines the minimum speed,

the front is known as *pulled*. In contrast, in *pushed* fronts, the minimum speed is given by a nonlinear criterion [18].

Due to the weak nonlinearity of the model, eq. (1), one expects that the linear criterion dictates the front speed [18,26]. To compute the minimal front speed, we consider the following ansatz for the  $\pi$ -kink tail:

$$\theta_i(t) = \pi + A_0 e^{(\alpha t - 2i\beta)} [1 + f_{\kappa;i}^\omega(t)], \quad (4)$$

where  $A_0 \ll 1$  is a small constant that characterizes the shape of the front tail, the index  $i$  is a positive and large integer number,  $\alpha \equiv K\langle v \rangle$ ,  $\beta \equiv K/2\sqrt{\kappa}$ , and  $K$  are parameters.  $f_{\kappa;i}^\omega(t)$  is a periodic function of frequency  $\omega$  in the  $i$ -th position of the chain that describes the oscillatory behavior of the speed. The numerical characterization of the amplitude of this function, is illustrated in fig. 3(c). In addition,  $f_{\kappa;i}^\omega(t) \rightarrow 0$  when  $i \rightarrow \infty$ . Introducing the above ansatz in eq. (1) and taking into account only the linear leading terms and dividing by the factor  $A_0^{-1}e^{-(\alpha t - 2i\beta)}$ , we obtain,

$$\begin{aligned} \ddot{\theta}_i A_0^{-1} e^{-(\alpha t - 2i\beta)} &= \alpha^2 [1 + f_{\kappa;i}^\omega] + 2\alpha \dot{f}_{\kappa;i}^\omega + \ddot{f}_{\kappa;i}^\omega \\ &= \omega^2 [1 + f_{\kappa;i}^\omega] - \mu \left[ \alpha [1 + f_{\kappa;i}^\omega] + \dot{f}_{\kappa;i}^\omega(t) \right] \\ &+ 4\kappa \sinh^2(\beta) + \kappa (e^{-2i\beta} f_{\kappa;i+1}^\omega - 2f_{\kappa;i}^\omega + e^{2i\beta} f_{\kappa;i-1}^\omega). \end{aligned} \quad (5)$$

Integrating this expression in a normalized period  $T = 2\pi/\omega$ , introducing the notation

$$\langle g(t) \rangle \equiv \frac{\omega}{2\pi} \int_0^{2\pi/\omega} g(t) dt, \quad (6)$$

and using the fact that  $\langle f_{\kappa;i}^\omega(t) \rangle = \langle \dot{f}_{\kappa;i}^\omega(t) \rangle = \langle \ddot{f}_{\kappa;i}^\omega(t) \rangle = 0$ , after straightforward calculations, we obtain  $\alpha^2 = \omega^2 - \mu\alpha + 4\kappa \sinh^2(\beta)$ . Substituting the definition of  $\alpha$ , the mean speed reads

$$\langle v \rangle = -\frac{\mu}{K} + \frac{1}{K} \sqrt{\mu^2 + \omega^2 + \frac{K^2}{\beta^2} \sinh^2(\beta)}, \quad (7)$$

and replacing  $K = 2\beta\sqrt{\kappa}$ ,

$$\langle v \rangle = -\frac{\mu}{2\beta\sqrt{\kappa}} + \frac{1}{2\beta} \sqrt{\kappa(\mu^2 + \omega^2) + 4\sinh^2(\beta)}. \quad (8)$$

The above expression accounts for the front mean speed as a function of the steepness ( $\beta$ ). In order to deduce the minimal mean front speed  $\langle v \rangle_{min}$ , we differentiate the above speed with respect to  $\beta$  and we get

$$\begin{aligned} \omega^2 (\mu^2 + \omega^2) \kappa^2 + 16 \sinh^2 \beta [\sinh \beta - \beta \cosh \beta]^2 = \\ -4 [(\mu^2 + 2\omega^2) \sinh^2 \beta - (\mu^2 + \omega^2) \beta \sinh 2\beta] \kappa. \end{aligned} \quad (9)$$

This expression gives us a relation between the critical steepness  $\beta_c$  and the coupling parameter  $\kappa$  or discretization parameter  $dx \equiv 1/\sqrt{\kappa}$ . An explicit expression  $\beta_c(dx)$  cannot be derived. Using expression (9) in formula (8), we obtain  $\langle v \rangle_{min}$  for the damped Frenkel-Kontorova model,

eq. (1). Note that this analytical result has a quite fair agreement with the numerical simulations as it is shown in fig. 2(a). Therefore, the asymptotic procedure is a suitable method to characterize the mean properties of front propagation, that is, the linear criterion determines the minimum mean speed of propagation of the  $\pi$ -kink solutions.

**Effective continuous description.** – Due to the complexity of discrete nature of the system under study, to obtain analytical results is a daunting task. Unlike continuous homogeneous systems, fronts in periodic media are characterized by a pulsating behavior as they propagate [27–30]. To figure out the oscillatory behavior of  $\pi$ -kinks, we consider an effective continuous equation with spatial periodic coefficients that accounts for the dynamics of the coupled system, analogously to the strategy proposed in ref. [27]. The benefit of this approach is that analytical calculations are accessible, which allows developing an intuitive understanding of the phenomenon.

Let us consider the continuous variable  $\theta(x, t)$ , which satisfies a modified sine-Gordon equation

$$\mu \partial_t \theta = -\frac{\delta \mathcal{F}}{\delta \theta}, \quad (10)$$

where the Lyapunov functional has the form

$$\mathcal{F} = \int \left[ \frac{1}{2} (\partial_t \theta)^2 + \omega^2 \cos \theta + (\partial_x \theta)^2 \left( \frac{D}{2} + \Gamma_{dx}(x) \right) \right] dx, \quad (11)$$

$\Gamma_{dx}(x)$  is a spatial periodic function with  $dx$  period, *i.e.*  $\Gamma_{dx}(x + dx) = \Gamma_{dx}(x)$ . This function accounts for the discreteness effect. The last term of the free energy is a generalization of the Peierls-Nabarro potential. This effective potential has been used to explain the dynamics of defects position such as dislocations in condensed matter physics or dynamics of the position of kink or fronts (see [12] and reference therein). The effective continuous equation of the damped Frenkel-Kontorova model for the field  $\theta(x, t)$  reads

$$\partial_{tt} \theta = \omega^2 \sin \theta - \mu \partial_t \theta + (D + 2\Gamma_{dx}) \partial_{xx} \theta + 2\Gamma'_{dx} \partial_x \theta. \quad (12)$$

This model corresponds to a sine-Gordon model with a linear damping, inhomogeneous diffusion and drift force.  $D$  accounts for the diffusion coefficient. Numerical simulations with a harmonic potential  $\Gamma_{dx}$  display  $\pi$ -kink solutions. These numerical simulations have been conducted with a discretized Laplacian and gradient of  $\theta$  to nearest neighbors considering a small discretization parameter. Figure 4 shows the profile of  $\pi$ -kink solution of eq. (12), propagating into an unstable state. The effective force,  $f \equiv 2\Gamma_{dx}(x) \partial_{xx} \theta + 2\Gamma'_{dx}(x) \partial_x \theta$  and the amplitude speed ( $\eta$ ) are also depicted. From this figure, we infer that the effective force  $f$  has higher amplitude oscillations about the region where the larger spatial variation of the  $\pi$ -kink takes place. Note that spatiotemporal diagrams of the effective continuous model, eq. (12), and the damped Frenkel-Kontorova model, eq. (1), possess similar qualitative dynamical behaviors. Moreover, we observe that the

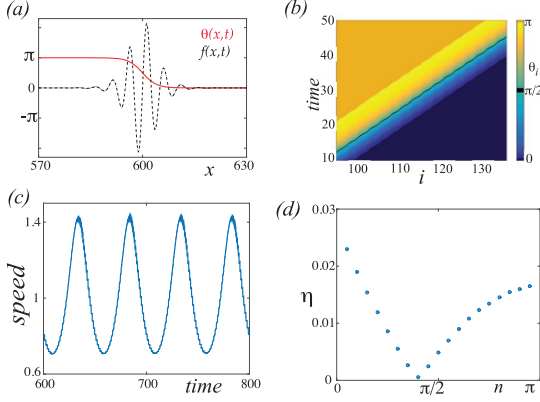


Fig. 4: (Color online)  $\pi$ -kink propagation in the effective damped Frenkel-Kontorova model, eq. (12) with a harmonic generalized Peierls-Nabarro potential,  $\Gamma_{dx}(x) = A \cos(2\pi x/dx)$  with  $\omega = 1.0$ ,  $D = 2.17$ ,  $\mu = 2.0$ ,  $A = 0.03$ , and  $dx = 5.0$ . The numerical discretization parameter of the finite differences method is 0.1. (a)  $\pi$ -kink solution and effective force  $f \equiv 2\Gamma_{dx}(x)\partial_{xx}\theta + 2\Gamma'_{dx}(x)\partial_x\theta$ . (b) Spatiotemporal diagram of  $\pi$ -kink propagation with same parameters but  $A = 1.0$ . (c) Temporal evolution of the  $\pi$ -kink speed  $v$ . (d) Oscillation amplitude of the  $\pi$ -kink speed,  $\eta$ , in different cuts.

structure of the oscillation amplitude of the speed is similar to that seen in the discrete case (cf. figs. 3(c) and 4(d)).

In the continuous limit  $dx \rightarrow 0$ , the effective force must be suppressed,  $\Gamma_{dx}(x) \rightarrow 0$ . Hence, the last two terms of eq. (12) are of perturbative nature. Under this assumption, analytical results are attainable. The damped sine-Gordon model, eq. (12) with  $\Gamma_{dx} = 0$ , has  $\pi$ -kink solutions of the form  $\theta_\pi(x - vt - p)$ , where  $p$  is a constant that accounts for the front position and  $v$  the front speed. Analytical expressions of these solutions are unknown. Proposing the following ansatz for large values of the coupling

$$\theta(x, t) = \theta_\pi(x - vt - p(t)) + w(x - vt - p), \quad (13)$$

where the front position is promoted to a temporal function  $p(t)$  and  $w$  is a small corrective function of the order of the perturbative force. Introducing the above ansatz in eq. (12) and linearizing in  $w$ , after straightforward calculations, we obtain

$$\begin{aligned} \mathcal{L}w = & \dot{p}(t)\partial_\xi\theta_\pi - (2v\partial_{\xi\xi}\theta_\pi - \mu\partial_\xi\theta_\pi)\dot{p}(t) \\ & - 2\Gamma_{dx}(x)\partial_{\xi\xi}\theta_\pi + 2\Gamma'_{dx}(x)\partial_\xi\theta_\pi, \end{aligned} \quad (14)$$

where  $\mathcal{L} \equiv -(D - v^2)\partial_{\xi\xi} - \mu v\partial_\xi - \omega^2 \cos\theta_\pi$  is a linear operator and  $\xi = x - vt - p$  is the coordinate in the co-mobile system. Considering the inner product  $\langle f|g \rangle \equiv \int_{-L}^L f(\xi)g(\xi)d\xi$ , where  $2L$  is the system size. To solve linear eq. (14), we apply the Fredholm alternative or the solvability condition [15], and obtain at dominate order

$$\dot{p}(t) = 2 \frac{\langle \Gamma_{dx}(\xi + vt + p)\partial_{\xi\xi}\theta_\pi|\psi \rangle}{\mu \langle \partial_\xi\theta_\pi|\psi \rangle} + 2 \frac{\langle \Gamma'_{dx}\partial_\xi\theta_\pi|\psi \rangle}{\mu \langle \partial_\xi\theta_\pi|\psi \rangle}, \quad (15)$$

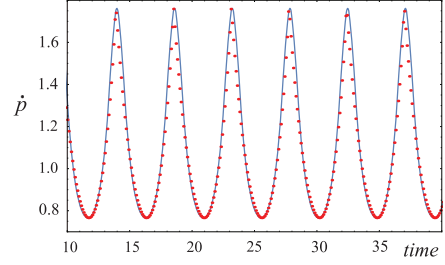


Fig. 5: (Color online)  $\pi$ -kink speed  $\dot{p}$  vs. time obtained from model, eq. (1). Dots correspond to numerical values of the  $\pi$ -kink speed, eq. (1), with  $\omega = 1$ ,  $\mu = 2.0$ , and  $\kappa = 0.04$ . The continuous line stands for the fitting curve of the  $\pi$ -kink speed using formula (18), with  $a = 0.631$ ,  $b = 0.680$ ,  $c = 3.0$ ,  $d = 0.550$ , and  $g = 0.358$ .

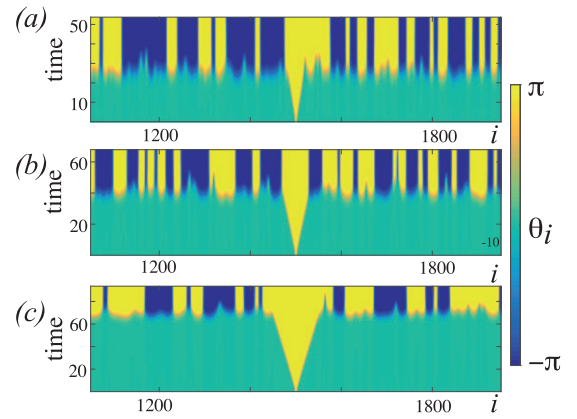


Fig. 6: (Color online) Fronts propagation into an unstable state in the noisy Frenkel-Kontorova model with dissipation. The system is perturbed with the same initial condition and with different noise levels intensity (a)  $\eta = 10^{-5}$ , (b)  $\eta = 10^{-10}$ , and (c)  $\eta = 10^{-20}$ .

where  $\psi(\xi)$  is an element of kernel of  $\mathcal{L}$  adjoint,  $\mathcal{L}^\dagger \equiv -(D - v^2)\partial_{\xi\xi} + \mu v\partial_\xi - \omega^2 \cos\theta_\pi$ , i.e.,  $\mathcal{L}^\dagger\psi = 0$ . The  $\psi$  function is unknown analytically. However, it diverges exponentially with the same exponent as  $\theta_\pi(\xi)$  converges to its equilibrium. Therefore the above integrals diverge proportional to  $L$ , however the ratio is well defined because  $\langle \partial_\xi\theta_\pi|\psi \rangle \sim L$ .

To understand the dynamics described by the above equation, we shall consider, for simplicity,  $\Gamma_{dx}(x) = \gamma(x) \equiv A \cos(2\pi x/dx)$ . Replacing this expression in eq. (15) and after straightforward calculations, we obtain

$$\dot{p}(t) = \sqrt{K_1^2 + K_2^2} \cos\left(\frac{2\pi}{dx}(p + vt) + \phi_0\right), \quad (16)$$

with

$$K_1 = A \frac{\left\langle \cos\left(\frac{2\pi\xi}{dx}\right) \partial_{\xi\xi}\theta_\pi - \frac{2\pi\xi}{dx} \sin\left(\frac{2\pi\xi}{dx}\right) \partial_\xi\theta_\pi|\psi \right\rangle}{\mu \langle \partial_\xi\theta_\pi|\psi \rangle},$$

$$K_2 = -A \frac{\left\langle \sin\left(\frac{2\pi\xi}{dx}\right) \partial_{\xi\xi}\theta_\pi + \frac{2\pi\xi}{dx} \cos\left(\frac{2\pi\xi}{dx}\right) \partial_\xi\theta_\pi \middle| \psi \right\rangle}{\mu \langle \partial_\xi\theta_\pi | \psi(\xi) \rangle},$$

$$\tan(\phi_0) = \frac{K_1}{K_2}. \quad (17)$$

Equation (16) can be rewritten in the following form:

$$\dot{p} = \frac{a}{1 + d \cos(bt + c)} + g, \quad (18)$$

where  $a$ ,  $b$ ,  $c$ ,  $d$ , and  $g$  are complicated functions of parameters  $\mu$ ,  $A$ , and  $dx$ . Therefore, the kink position propagates in an oscillatory manner, that is, consistent with numerical observation. Figure 5 compares the numerical  $\pi$ -kink speed of model (1) with the fitting curve formula (18). The analytical result is in a good agreement with the observed dynamics. Hence, the dynamics of model (1) can be understood using a continuous model with an effective potential, eq. (12).

**Conclusions and remarks.** – We have studied kink propagation into an unstable state in the Frenkel-Kontorova model with dissipation, which is a prototype model of nonlinear waves propagation in discrete media. We reveal that  $\pi$ -kink propagation occurs in an oscillatory manner. Different parts of the  $\pi$ -kink oscillate with the same frequency but different amplitude. However, the whole structure possesses the same average speed. The amplitude of the oscillation is minimal at the front position, increases as one moves away from the front position and decays to zero abruptly in the tails. The asymptotic behavior of this propagation allows us to determine the minimum mean speed analytically. To describe this latter phenomenon, we generalize the notion of the Peierls-Nabarro potential, which makes it possible to have an effective continuous description of the system. Numerical simulations show quite fair agreement between the Frenkel-Kontorova model and the effective continuous system. Fronts in coupled oscillators have also been studied in the context of the discrete nonlinear Schrödinger equation with internal losses [19]. In the studied parameter region, of small loss, the coefficient of dispersion is of order one. On the other hand, when the dispersion is not considered, the losses are of order one or greater. In both cases, shock waves propagate with constant speed, and no oscillatory behavior is observed, being well-described by the continuous limit. Considering weak diffusion and dispersion shock waves should propagate with oscillatory velocity and exhibit an internal dynamics as it is observed in  $\pi$ -kink propagation in discrete media.

Stochastic equations give a more realistic description of macroscopic systems. The inherent fluctuations are responsible for triggering the blow-up of unstable states, giving rise to fronts propagation and domain walls. The creation of domain walls can inhibit the observation of fronts. Figure 6 shows a front propagation into an unstable state in the stochastic dissipative Frenkel-Kontorova model. We consider an additive white-noise term with

intensity  $\eta$ . Linearizing around the unstable state, one can estimate the propagation period of the front as  $\tau = -\log(\eta)/\lambda$  with  $\lambda = [-\mu + \sqrt{\mu^2 + 4\omega^2}]/2$ , where the initial condition is considered of the order of the noise intensity. Namely, as a result of fluctuations, the front can only propagate for a short period  $\tau$  proportional to the logarithmic of noise intensity (see fig. 6).

Further understanding of the propagation of nonlinear waves in optically coupled oscillators may allow novel and fresh ways of manipulating light at micrometrical scales [23].  $\pi$ -kinks propagation in two dimensions is affected by the curvature of the interface, which can increase or decrease the speed of the propagating interface. Studies of fronts propagation into unstable states in these contexts are in progress.

\*\*\*

MGC, MAG-N, and RGR acknowledge the financial support of FONDECYT projects 1150507, 11130450, and 1130622, respectively. KA-B was supported by CONICYT, scholarship Beca de Doctorado Nacional No. 21140668.

## REFERENCES

- [1] FROVA A. and MARENZANA M., *Thus Spoke Galileo: The Great Scientist's Ideas and their Relevance to the Present Day* (Oxford University Press) 2006.
- [2] BAKER G. L. and BLACKBURN J. A., *The Pendulum: A Case Study in Physics* (Oxford University Press) 2005.
- [3] PIKOVSKY A., ROSENBLUM M. and KURTHS J., *Synchronization: A Universal Concept in Nonlinear Sciences* (Cambridge University Press, Cambridge) 2001.
- [4] KURAMOTO Y., *Chemical Oscillations, Waves, and Turbulence* (Springer-Verlag, Berlin, Heidelberg) 1984.
- [5] KANEKO K. and TSUDA I., *Chaos and Beyond: A Constructive Approach with Applications in Life Sciences* (Springer, Berlin) 1996.
- [6] SHRAIMAN B. I., PUMIR A., VAN SAARLOOS W., HOHENBERG P. C., CHATE H. and HOLEN M., *Physica D*, **57** (1992) 241.
- [7] NEWELL A. C., RAND D. A. and RUSSELL D., *Physica D*, **33** (1988) 281.
- [8] COULLET P., GIL L. and LEGA J., *Phys. Rev. Lett.*, **62** (1989) 1619.
- [9] CHATE H., *Nonlinearity*, **7** (1994) 185.
- [10] CLERC M. G. and VERSCHUEREN N., *Phys. Rev. E.*, **88** (2013) 052916.
- [11] CLERC M. G., COULIBALY S., FERRÉ M. A., GARCÍA-ÑUSTES M. A. and ROJAS R. G., *Phys. Rev. E*, **93** (2016) 052204.
- [12] BRAUN O. M. and KIVSHAR Y., *The Frenkel-Kontorova Model: Concepts, Methods, and Applications* (Springer-Verlag, Berlin, Heidelberg) 2004.
- [13] KONTOROVA T. A. and FRENKEL Y. I., *Zh. Eksp. Teor. Fiz.*, **8** (1938) 1340.
- [14] KIVSHAR Y. S., GRONBECH-JENSEN N. and SAMUELSEN M. R., *Phys. Rev. B*, **45** (1992) 7789.

- [15] PISMEN L. M., *Patterns and Interfaces in Dissipative Dynamics Springer Series in Synergetics* (Springer, Berlin, Heidelberg) 2006.
- [16] CROSS M. and GREENSIDE H., *Pattern Formation and Dynamics in Nonequilibrium Systems* (Cambridge University Press, New York) 2009.
- [17] CLERC M. G., NAGAYA T., PETROSSIAN A., RESIDORI S. and RIERA C. S., *Eur. Phys. J. D*, **28** (2004) 435.
- [18] VAN SAARLOOS W., *Phys. Rep.*, **386** (2003) 29.
- [19] SALERNO M., MALOMED B. A. and KONOTOP V. V., *Phys. Rev. E*, **62** (2000) 8651.
- [20] LANGER J. S., *Rev. Mod. Phys.*, **52** (1980) 1.
- [21] COLLET P. and ECKMANN J. P., *Instabilities and Fronts in Extended Systems* (Princeton University Press, Princeton) 2014.
- [22] BARBAY S., SAGNES I., KUSZELEWICZ R. and YACOMOTTI A. M., in *2011 Fifth Rio De La Plata Workshop on Laser Dynamics and Nonlinear Photonics* (IEEE) 2011.
- [23] SELMI F., PhD. Thesis, University of Paris-Sud (2015), <https://tel.archives-ouvertes.fr/tel-01199595/document>.
- [24] CUEVAS-MARAVAR J., KEVREKIDIS P. G. and WILLIAMS F., *The sine-Gordon Model and its Applications* (Springer) 2014.
- [25] BENNETT D., BISHOP A. and TRULLINGER S., *Z. Phys. B-Condens. Matter*, **47** (1982) 265.
- [26] KOLMOGOROFF A., PETROVSKY I. and PISCOUNOFF N., in *Dynamics of Curved Fronts*, edited by PELCÉ P. (Academic Press, London) 2012, p. 105.
- [27] CLERC M. G., ELÍAS R. G. and ROJAS R. G., *Philos. Trans. R. Soc. A*, **369** (2011) 412.
- [28] HAMEL F., *J. Math. Pures Appl.*, **89** (2008) 355.
- [29] HAUDIN F., ELÍAS R. G., ROJAS R. G., BORTOLOZZO U., CLERC M. G. and RESIDORI S., *Phys. Rev. Lett.*, **103** (2009) 128003.
- [30] HAUDIN F., ELÍAS R. G., ROJAS R. G., BORTOLOZZO U., CLERC M. G. and RESIDORI S., *Phys. Rev. E*, **81** (2010) 056203.